Nanostructures

DOI: 10.1002/anie.201104943

Anisotropic Growth of Titania onto Various Gold Nanostructures: Synthesis, Theoretical Understanding, and Optimization for Catalysis

Zhi Wei Seh, Shuhua Liu, Shuang-Yuan Zhang, M. S. Bharathi, H. Ramanarayan, Michelle Low, Kwok Wei Shah, Yong-Wei Zhang, and Ming-Yong Han**

Dedicated to the Fritz Haber Institute, Berlin, on the occasion of its 100th anniversary

To incorporate new functionalities, various oxide-based materials are being combined with metal nanoparticles to form metal–oxide hybrid nanostructures for a wide range of promising applications, including labeling/sensing,[1] catalysis,[2,3] and surface-enhanced Raman scattering.[4] Over the years, many efforts have been devoted to the growth of inert protective SiO_2 shells onto metal cores to form concentric core–shell nanostructures.[5,6] It is of great interest to couple metal nanoparticles with other oxides (e.g., TiO_2,[7] CeO_2,[2] Fe_3O_4[8]) to form non-centrosymmetric metal–oxide nanostructures with combined optical, catalytic, and magnetic properties. In particular, the Janus/heterodimer geometry is gaining importance because it couples two or more dissimilar components at a small junction, exposing the other regions for optimal expression of their combined functionalities.[9] Common strategies used to achieve the Janus/heterodimer geometry include cation exchange,[10] site-selective nucleation,[11] direct epitaxial growth,[8,12] and nonepitaxial growth due to lattice mismatch.[13] However, many of the Janus structures reported in the literature are chalcogenide-based, and studies on the growth of oxide-based materials onto metal cores to form Janus nanostructures are still very limited.[9]

Herein, we have report the successful control of the anisotropic growth of TiO_2 onto spherical gold nanoparticles, short gold nanorods, and long gold nanorods, and the three different resulting geometries for each of them, namely, Janus, eccentric core–shell, and concentric core–shell geometries. By using theoretical energy calculations to study the balance between interfacial and elastic energies, we have provided the first understanding that the Janus and concentric geometries are both energetically stable structures formed by varying the volume and mode of addition of the precursor, whereas the eccentric geometry represents a metastable state. The unique advantage of the energetically stable Janus geometry lies in the exposure of the gold core on one side, which provides direct access to reactants for high catalytic rates. We have demonstrated that the Janus TiO_2-coated spherical gold nanoparticles showed a catalytic activity as fast as that of bare gold nanoparticles during the first cycle of use. Moreover, the Janus Au-TiO_2 nanostructures possessed long-term stability over multiple cycles due to the presence of protective TiO_2 coatings, unlike bare gold nanoparticles, which suffered from irreversible aggregation.

Experimentally, spherical gold nanoparticles approximately 50 nm in size were prepared using seed-mediated growth in the presence of citrate ions (Figure S2a, Supporting Information),[14a] and they were subsequently stirred overnight with a stabilizing agent (hydroxypropyl cellulose, $M_w \approx 370\,000$) prior to TiO_2 coating. Short and long gold nanorods (aspect ratios ca. 3.5 and 16, respectively) were also synthesized using seed-mediated growth in the presence of cetyl trimethylammonium bromide (CTAB, Figure S2b,c, Supporting Information).[14b,c] The as-synthesized gold nanorods were purified by centrifugation to remove free CTAB and spherical side products, hydroxypropyl cellulose solution was subsequently added. After stirring overnight, CTAB on the gold nanorods was successfully exchanged with hydroxypropyl cellulose, as evidenced by Fourier transform infrared spectroscopy (Figure S3, Supporting Information). To control the coating of TiO_2 onto the hydroxypropyl cellulose-capped gold cores, we used a titanium diisopropoxide bis(acetylacetonate) precursor, which has a much slower hydrolysis rate than conventional precursors such as titanium tetrabutoxide. This procedure helps to separate nucleation and growth of TiO_2, leading to the geometry-controlled synthesis of uniform Au-TiO_2 nanostructures.

First, we examined the growth of TiO_2 onto short gold nanorods because their shapes and dimensions are more well-defined as compared to spherical nanoparticles and long nanorods. The geometry of the TiO_2-coated short gold nanorods can be tuned by controlling the volume and mode of addition of the titanium diisopropoxide bis(acetylacetonate) precursor (TDAA, 10 mM in isopropyl alcohol). Typically, the TDAA precursor solution was added to a reaction mixture (pH 9–10) containing ammonia (25 wt%, 3 mL), isopropyl alcohol (100 mL), and as-prepared gold nanorods (25 mL), with subsequent shaking for 20 h at room temperature. When 3 mL of the TDAA precursor solution was added in one portion, TiO_2 was found to grow anisotropically on one

[*] Z. W. Seh, Dr. S. H. Liu, S. Y. Zhang, M. Low, K. W. Shah, Prof. M. Y. Han
Institute of Materials Research and Engineering
Agency for Science, Technology and Research (A*STAR)
3 Research Link, Singapore 117602 (Singapore)
E-mail: my-han@imre.a-star.edu.sg
Dr. M. S. Bharathi, Dr. H. Ramanarayan, Prof. Y. W. Zhang
Institute of High Performance Computing, A*STAR
1 Fusionopolis Way, Singapore 138632 (Singapore)
E-mail: zhangyw@ihpc.a-star.edu.sg
Prof. M. Y. Han
Division of Bioengineering, National University of Singapore
Singapore 117576 (Singapore)

Supporting information for this article is available on the WWW under http://dx.doi.org/10.1002/anie.201104943.

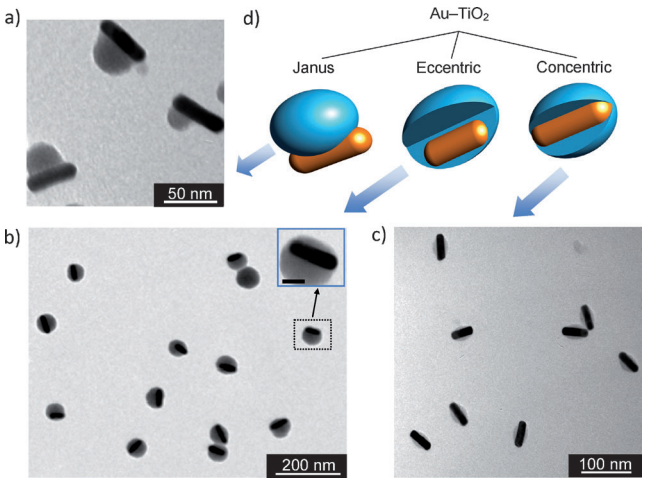

Figure 1. a–c) TEM images of TiO_2-coated short gold nanorods with a) Janus, b) eccentric, and c) concentric geometries, which were prepared by adding TDAA (3 mL) in one portion, TDAA (3 mL) in three portions, and TDAA (9 mL) in three portions, respectively. The inset in (b) shows a thinner TiO_2 shell on one side and a thicker one on the opposite side (scale bar = 25 nm). d) Schematic representations of the TiO_2-coated short gold nanorods with various geometries.

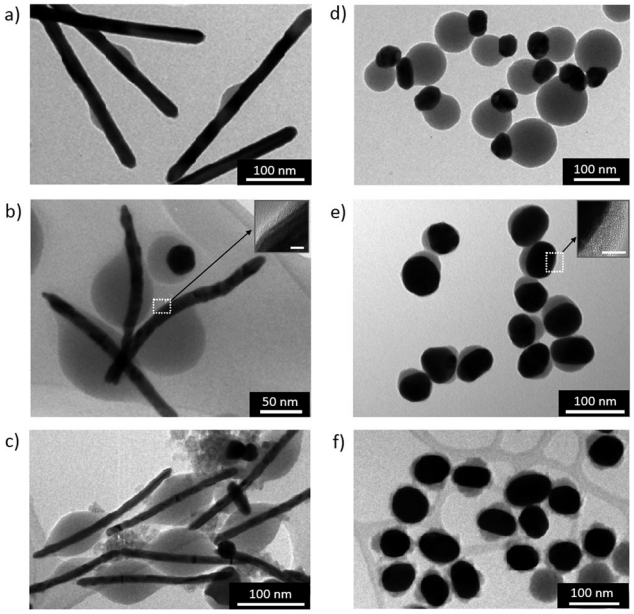

Figure 2. a–c) TEM images of TiO_2-coated long gold nanorods with a) Janus, b) eccentric, and c) concentric geometries. d–f) TEM images of TiO_2-coated spherical gold nanoparticles with d) Janus, e) eccentric, and f) concentric geometries. The various geometries were prepared using the same volume and mode of addition of the TDAA precursor as in the case of short gold nanorods. Insets in (b) and (e) show the thinner TiO_2 shell on one side of the gold core (scale bars = 5 nm).

side of the nanorods, leaving the other side exposed, forming Janus TiO_2-coated short gold nanorods (Figure 1a). In comparison, when 3 mL of the precursor solution was added in three portions (3×1 mL) at one-hour intervals, the nanorods were encapsulated by a thinner TiO_2 shell on one side and a thicker one on the opposite side, forming the eccentric geometry (Figure 1b; see also Figure S4, Supporting Information). Finally, when a larger volume (9 mL) of the precursor solution was added in three portions (3×3 mL) at one-hour intervals, concentric Au-TiO_2 nanostructures, with uniformly thick shells on both sides of the gold nanorods, were formed instead (Figure 1c). We also note that when 9 mL of the precursor solution was added in one portion, the Janus geometry was formed, accompanied by a large amount of free TiO_2 nanoparticles in solution. In all cases, the TiO_2 coatings on the gold nanorods were found to be amorphous.

To further investigate the anisotropic growth of TiO_2, long gold nanorods were used for TiO_2 coating as well. We can also tune the geometry of TiO_2-coated long gold nanorods from Janus (Figure 2a) to eccentric (Figure 2b) to concentric (Figure 2c), using the same volume and mode of addition of the TDAA precursor as in the case of short gold nanorods. In the Janus geometry, the TiO_2 coating is not thick enough to cause noticeable bending of the long gold nanorods (Figure 2a). As the thickness of the TiO_2 coating is increased in the eccentric case, we can see clearly that the nanorods are bent towards the side with the thicker TiO_2 shell (Figure 2b), indicating the presence of elastic energy in the nanorods. On the other hand, in the concentric case, we only observed slight bending of the nanorods (Figure 2c), indicating minimal elastic energy. By using the same volume and mode of addition of the TDAA precursor as in the case of short gold nanorods, we can also synthesize TiO_2-coated spherical gold nanoparticles with Janus (Figure 2d), eccentric (Figure 2e), and concentric (Figure 2f) geometries.

Using theoretical energy calculations, we investigated the geometry-controlled synthesis of the various Au-TiO_2 nanostructures, which is highly dependent on the volume and mode of addition of the TDAA precursor. The formation of the three different Au-TiO_2 geometries can be understood by examining the competition between interfacial energy and elastic energy. The geometry of the Au-TiO_2 nanostructures is influenced by the balance between the gold surface energy (γ_{gold}), TiO_2 surface energy (γ_{TiO_2}) and gold-TiO_2 interfacial energy ($\gamma_{gold\text{-}TiO_2}$; Figure 3a). We let the length of the TiO_2 shell be L_1 and L_2 on each side of the gold nanorod of length L (Figure 3a). The growth of TiO_2 on the gold nanorod can either be on one side (Janus, $L_1/L_2 = 0$), distributed equally on

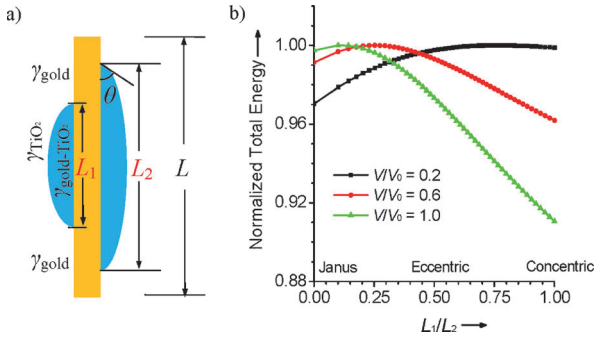

Figure 3. a) Schematic representation of the model of a TiO_2-coated gold nanorod used for theoretical energy calculations. b) Plots of normalized total energy (sum of interfacial and elastic energies) of the system versus L_1/L_2 for various values of $V/V_0 = (L_1^2 + L_2^2)/2L^2$, which is related to the volume of TDAA precursor solution added.

both sides (concentric, $L_1/L_2 = 1$), or distributed unequally on both sides (eccentric, $0 < L_1/L_2 < 1$). When the TiO_2 shell is distributed unequally on either or both sides of the gold nanorod, the unbalanced forces would cause bending of the nanorod, thus leading to an increase in elastic energy. Using theoretical calculations, we studied the normalized total energy (sum of interfacial and elastic energies) of the system as a function of L_1/L_2 for various values of V/V_0 (0.2, 0.6, and 1.0), where $V/V_0 = (L_1^2 + L_2^2)/2L^2$ represents the normalized total volume of TiO_2 formed on the gold nanorod, which is related to the volume of TDAA precursor solution added (see the Supporting Information for details).

From the results of the theoretical calculations in Figure 3b, we see that when $V/V_0 = 0.2$, the minimum in total energy occurs at $L_1/L_2 = 0$, which corresponds to the Janus geometry. This finding indicates that when a smaller volume of the TDAA precursor solution is added (e.g., 3 mL in one portion), the Janus geometry is the most energetically stable configuration, which is consistent with experimental observations. Since the partially hydrolyzed TDAA precursor is hydrophobic in nature, it does not have good wettability on the hydrophilic surface of the hydroxypropyl cellulose capped gold nanorods. As a result, the TiO_2 would nucleate and grow on one side of the gold nanorods to reduce the Au-TiO_2 interfacial area, thus enabling minimization of interfacial energy at the expense of elastic energy due to bending of the nanorods. The results of the theoretical calculations also indicate that, while the Janus geometry is an energetically stable structure, the eccentric geometry represents a metastable state (Figure 3b). To confirm this point, the eccentric TiO_2-coated short gold nanorods were synthesized using the same conditions, except that the reaction was allowed to continue for a longer period of time (100 h instead of the usual 20 h). It was found that the thinner side of the TiO_2 shell became thinner while the thicker side became thicker (Table S1, Supporting Information), which indicates that the metastable eccentric geometry approaches the energetically stable Janus geometry as a result of ripening.

In contrast, when V/V_0 is increased to 0.6 or 1.0, the minimum in total energy occurs at $L_1/L_2 = 1$, which corresponds to the concentric geometry (Figure 3b). This finding indicates that when a larger volume of the TDAA precursor solution is added (e.g., 9 mL in three portions), the concentric geometry becomes the most energetically stable configuration, which is consistent with our experimental results as well. The addition of a larger amount of precursor in three rather than one portion reduces the amount of precursor that would self-nucleate and grow to form free TiO_2 nanoparticles. This approach helps to maintain a high concentration of the precursor in solution, making it equally possible for TiO_2 to nucleate and grow on both sides of the gold nanorods to form the concentric geometry. In this case, although an additional Au-TiO_2 interface is formed, bending of the nanorods does not occur, allowing minimization of elastic energy at the expense of interfacial energy. Finally, we note that when 9 mL of the TDAA precursor solution was added in one portion, a large amount of the precursor self-nucleated and grew in solution to form free TiO_2 nanoparticles because of the high initial supersaturation, and the rest of the precursor with lower effective concentration nucleated and grew on one side of the gold nanorods to form the Janus geometry, as in the case when 3 mL of the precursor solution was added in one portion ($V/V_0 = 0.2$, Figure 3b).

The unique advantage of the Janus geometry lies in the exposure of the gold core on one side, which provides direct access to reactants for high catalytic rates. To study the catalytic activity of Janus TiO_2-coated spherical gold nanoparticles (Figure 2d), we used the reduction of 4-nitrophenol to 4-aminophenol by sodium borohydride,[3b,d] which is known to be catalyzed in the presence of gold (see the Supporting Information for details). In the absence of Au-TiO_2 catalysts, 4-nitrophenol was not reduced even after a period of 24 h. When the Janus TiO_2-coated spherical gold nanoparticles were added, the absorption intensity of 4-nitrophenol at 400 nm decreased quickly with time, accompanied by the formation of the reduction product 4-aminophenol ($\lambda =$ 300 nm), achieving 99% conversion in 6 min (Figure 4a). The rate constant was determined from the slope of the linear fit of $\ln(C_t/C_o)$ versus time, where C_t/C_o represents the ratio of 4-nitrophenol concentrations at time t and 0 as determined spectroscopically (Figure 4b). The Janus nanostructures were found to catalyze the reaction at a rate as fast as that of bare spherical gold nanoparticles during the first cycle of use (Figure 4b), because the exposed gold core on one side of the Janus catalysts provides direct access to 4-nitrophenol. Moreover, the Janus catalysts can be reused over five cycles with no obvious reduction in activity due to the presence of TiO_2

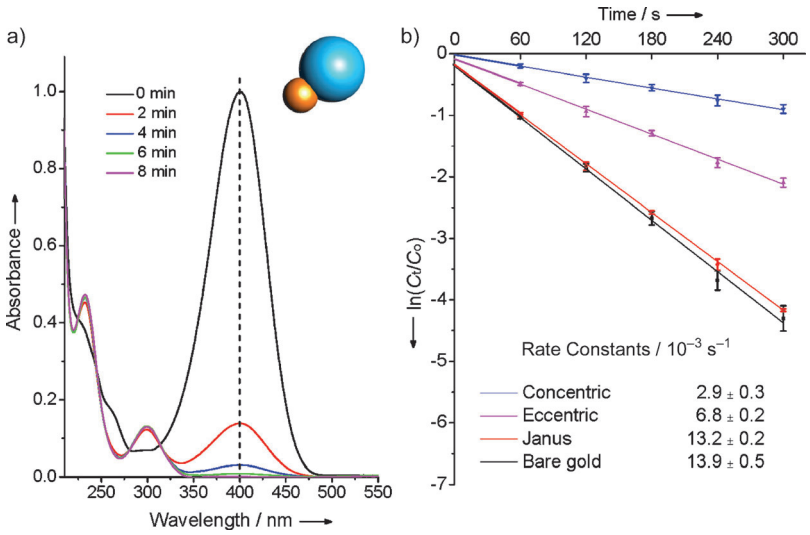

Figure 4. Catalytic reduction of 4-nitrophenol to 4-aminophenol by sodium borohydride during the first cycle of use. a) Time-dependent evolution of UV/Vis absorption spectra using the Janus TiO_2-coated spherical gold nanoparticles. b) Plots of $\ln(C_t/C_o)$ versus time and the rate constants for bare and TiO_2-coated spherical gold nanoparticles with various geometries. The concentration of catalysts used was kept constant at approximately 5.0×10^{10} particles mL^{-1} for all experiments.

coatings that protect against aggregation (Figure S5a,b, Supporting Information). In contrast, the catalytic activity of unprotected bare gold nanoparticles was reduced to almost zero at the end of five cycles due to irreversible aggregation (Figure S5a,c, Supporting Information). Upon comparing the catalytic activities of TiO_2-coated spherical gold nanoparticles with various geometries, we found that the rate constant for the Janus catalysts was twice that of the eccentric catalysts and 4.5 times that of the concentric ones (Figure 4b). This is because in the eccentric and concentric structures, 4-nitrophenol needs to diffuse through the encapsulating TiO_2 shell to reach the gold core for catalysis. We also demonstrate that the eccentric and concentric catalysts can be reused over five cycles with no obvious reduction in activity (Figure S6, Supporting Information). Further work is ongoing to investigate the catalytic rates and reusability of TiO_2-coated gold nanorods with various geometries.

In conclusion, we have introduced a facile method to tune the anisotropic growth of TiO_2 onto various gold nanostructures through a fine control of interfacial energy versus elastic energy. Using theoretical energy calculations, we have provided the first understanding that the Janus and concentric geometries are both energetically stable structures formed by varying the volume and mode of addition of the precursor, whereas the eccentric geometry represents a metastable state. Out of all three geometries, the energetically stable Janus nanostructures exhibited the highest catalytic activity because the exposed gold core on one side offers high accessibility to reactants, while the TiO_2 coating on the other side imparts protection against aggregation. This work provides us with insight on tuning the geometry of various Au-TiO_2 nanostructures, which can be extended to other metal–oxide composites to achieve optimal catalytic activity for various applications.

Received: July 15, 2011
Published online: September 13, 2011

Keywords: anisotropic growth · heterogeneous catalysis · gold · nanomaterials · titania

[1] a) S. H. Liu, Z. H. Zhang, M. Y. Han, *Anal. Chem.* **2005**, *77*, 2595 – 2600; b) S. H. Liu, Y. Wong, Y. B. Wang, D. S. Wang, M. Y. Han, *Adv. Funct. Mater.* **2007**, *17*, 3147 – 3152; c) C. Xue, X. Chen, S. J. Hurst, C. A. Mirkin, *Adv. Mater.* **2007**, *19*, 4071 – 4074.

[2] a) M. Cargnello, N. L. Wieder, T. Montini, R. J. Gorte, P. Fornasiero, *J. Am. Chem. Soc.* **2010**, *132*, 1402 – 1409; b) H. P. Zhou, H. S. Wu, J. Shen, A. X. Yin, L. D. Sun, C. H. Yan, *J. Am. Chem. Soc.* **2010**, *132*, 4998 – 4999.

[3] a) M. Haruta, M. Date, *Appl. Catal. A* **2001**, *222*, 427 – 437; b) J. Lee, J. C. Park, H. Song, *Adv. Mater.* **2008**, *20*, 1523 – 1528; c) E. I. Ross-Medgaarden, I. E. Wachs, W. V. Knowles, A. Burrows, C. J. Kiely, M. S. Wong, *J. Am. Chem. Soc.* **2009**, *131*, 680 – 687; d) Y. H. Deng, Y. Cai, Z. K. Sun, J. Liu, C. Liu, J. Wei, W. Li, Y. Wang, D. Y. Zhao, *J. Am. Chem. Soc.* **2010**, *132*, 8466 – 8473; e) Y. Zhu, H. F. Qian, B. A. Drake, R. C. Jin, *Angew. Chem.* **2010**, *122*, 1317 – 1320; *Angew. Chem. Int. Ed.* **2010**, *49*, 1295 – 1298; f) A. Mohanty, N. Garg, R. C. Jin, *Angew. Chem.* **2010**, *122*, 5082 – 5086; *Angew. Chem. Int. Ed.* **2010**, *49*, 4962 – 4966; g) C. Wen, Y. Liu, F. Tao, *Pure Appl. Chem.* **2011**, *83*, 243 – 252.

[4] a) W. E. Doering, S. M. Nie, *Anal. Chem.* **2003**, *75*, 6171 – 6176; b) M. Y. Sha, H. X. Xu, M. J. Natan, R. Cromer, *J. Am. Chem. Soc.* **2008**, *130*, 17214 – 17215.

[5] a) L. M. Liz-Marzán, M. Giersig, P. Mulvaney, *Langmuir* **1996**, *12*, 4329 – 4335; b) S. H. Liu, M. Y. Han, *Chem. Asian J.* **2010**, *5*, 36 – 45; c) A. Guerrero-Martínez, J. Pérez-Juste, L. M. Liz-Marzán, *Adv. Mater.* **2010**, *22*, 1182 – 1195.

[6] a) S. O. Obare, N. R. Jana, C. J. Murphy, *Nano Lett.* **2001**, *1*, 601 – 603; b) Y. Lu, Y. D. Yin, Z. Y. Li, Y. N. Xia, *Nano Lett.* **2002**, *2*, 785 – 788; c) C. Graf, D. L. J. Vossen, A. Imhof, A. van Blaaderen, *Langmuir* **2003**, *19*, 6693 – 6700; d) I. Gorelikov, N. Matsuura, *Nano Lett.* **2008**, *8*, 369 – 373.

[7] a) K. S. Mayya, D. I. Gittins, F. Caruso, *Chem. Mater.* **2001**, *13*, 3833 – 3836; b) J. Li, H. C. Zeng, *Angew. Chem.* **2005**, *117*, 4416 – 4419; *Angew. Chem. Int. Ed.* **2005**, *44*, 4342 – 4345; c) H. Sakai, T. Kanda, H. Shibata, T. Ohkubo, M. Abe, *J. Am. Chem. Soc.* **2006**, *128*, 4944 – 4945; d) S. Pradhan, D. Ghosh, S. W. Chen, *ACS Appl. Mater. Interfaces* **2009**, *1*, 2060 – 2065; e) A. F. Demirörs, A. van Blaaderen, A. Imhof, *Langmuir* **2010**, *26*, 9297 – 9303; f) Z. W. Seh, S. H. Liu, S. Y. Zhang, K. W. Shah, M. Y. Han, *Chem. Commun.* **2011**, *47*, 6689 – 6691.

[8] a) H. Yu, M. Chen, P. M. Rice, S. X. Wang, R. L. White, S. H. Sun, *Nano Lett.* **2005**, *5*, 379 – 382; b) W. L. Shi, H. Zeng, Y. Sahoo, T. Y. Ohulchanskyy, Y. Ding, Z. L. Wang, M. Swihart, P. N. Prasad, *Nano Lett.* **2006**, *6*, 875 – 881; c) Y. D. Jin, C. X. Jia, S. W. Huang, M. O'Donnell, X. H. Gao, *Nat. Commun.* **2010**, DOI: 10.1038/ncomms1042.

[9] a) H. W. Gu, Z. M. Yang, J. H. Gao, C. K. Chang, B. Xu, *J. Am. Chem. Soc.* **2005**, *127*, 34 – 35; b) H. K. Yu, Z. W. Mao, D. Y. Wang, *J. Am. Chem. Soc.* **2009**, *131*, 6366 – 6367; c) S. X. Xing, Y. H. Feng, Y. Y. Tay, T. Chen, J. Xu, M. Pan, J. T. He, H. H. Hng, Q. Y. Yan, H. Y. Chen, *J. Am. Chem. Soc.* **2010**, *132*, 9537 – 9539; d) T. Chen, G. Chen, S. X. Xing, T. Wu, H. Y. Chen, *Chem. Mater.* **2010**, *22*, 3826 – 3828; e) L. Carbone, P. D. Cozzoli, *Nano Today* **2010**, *5*, 449 – 493; f) R. Costi, A. E. Saunders, U. Banin, *Angew. Chem.* **2010**, *122*, 4996 – 5016; *Angew. Chem. Int. Ed.* **2010**, *49*, 4878 – 4897; g) J. K. Sahoo, M. N. Tahir, A. Yella, T. D. Schladt, E. Mugnaoli, U. Kolb, W. Tremel, *Angew. Chem.* **2010**, *122*, 7741 – 7745; *Angew. Chem. Int. Ed.* **2010**, *49*, 7578 – 7582.

[10] a) R. D. Robinson, B. Sadtler, D. O. Demchenko, C. K. Erdonmez, L. W. Wang, A. P. Alivisatos, *Science* **2007**, *317*, 355 – 358; b) M. D. Regulacio, C. Ye, S. H. Lim, M. Bosman, L. Polavarapu, W. L. Koh, J. Zhang, Q. H. Xu, M. Y. Han, *J. Am. Chem. Soc.* **2011**, *133*, 2052 – 2055.

[11] a) T. Mokari, C. G. Sztrum, A. Salant, E. Rabani, U. Banin, *Nat. Mater.* **2005**, *4*, 855 – 863; b) S. Chakrabortty, J. A. Yang, Y. M. Tan, N. Mishra, Y. T. Chan, *Angew. Chem.* **2010**, *122*, 2950 – 2954; *Angew. Chem. Int. Ed.* **2010**, *49*, 2888 – 2892; c) X. H. Li, J. Lian, M. Lin, Y. T. Chan, *J. Am. Chem. Soc.* **2011**, *133*, 672 – 675; d) S. Pal, R. Varghese, Z. T. Deng, Z. Zhao, A. Kumar, H. Yan, Y. Liu, *Angew. Chem.* **2011**, *123*, 4262 – 4265; *Angew. Chem. Int. Ed.* **2011**, *50*, 4176 – 4179.

[12] a) T. Pellegrino, A. Fiore, E. Carlino, C. Giannini, P. D. Cozzoli, G. Ciccarella, M. Respaud, L. Palmirotta, R. Cingolani, L. Manna, *J. Am. Chem. Soc.* **2006**, *128*, 6690 – 6698; b) J. S. Choi, Y. W. Jun, S. I. Yeon, H. C. Kim, J. S. Shin, J. Cheon, *J. Am. Chem. Soc.* **2006**, *128*, 15982 – 15983.

[13] a) K. W. Kwon, M. Shim, *J. Am. Chem. Soc.* **2005**, *127*, 10269 – 10275; b) M. Casavola, A. Falqui, M. A. Garcia, M. Garcia-Hernandez, C. Giannini, R. Cingolani, P. D. Cozzoli, *Nano Lett.* **2009**, *9*, 366 – 376.

[14] a) S. H. Liu, M. Y. Han, *Adv. Funct. Mater.* **2005**, *15*, 961 – 967; b) L. F. Gou, C. J. Murphy, *Chem. Mater.* **2005**, *17*, 3668 – 3672; c) B. D. Busbee, S. O. Obare, C. J. Murphy, *Adv. Mater.* **2003**, *15*, 414 – 416.

